ELSEVIER

PII: S0032-3861(97)10356-1

Polymer Vol. 39 No. 21, pp. 5027–5033, 1998
0032-3861/98/$ – see front matter

Effect of morphology on the brittle ductile transition of polymer blends: 3. The influence of rubber particle spatial distribution on the fracture behaviour of poly(vinyl chloride)/nitrile rubber blends

Z. H. Liu[a], X. D. Zhang†, X. G. Zhu[a], Z. N. Qi[a,*], F. S. Wang, R. K. Y. Li[b] and C. L. Choy

[a]*State Key Laboratory of Engineering Plastics, Institute of Chemistry, Chinese Academy of Sciences, Beijing 100080, People's Republic of China*
[b]*Department of Physics and Materials Science, City University of Hong Kong, Tat Chee Avenue, Kowloon, Hong Kong, People's Republic of China*
[c]*Department of Applied Physics, Hong Kong Polytechnic University, Hung Hom, Kowloon, Hong Kong, People's Republic of China*
(Received 6 June 1997; revised 30 September 1997; accepted 25 November 1997)

Poly(vinyl chloride) (PVC)/nitrile rubber (NBR) blends with the pseudonetwork morphology and the morphology of well-dispersed particles were prepared to elucidate the influence of rubber particle spatial distribution on the fracture behaviour of the blends. The main toughening mechanism of PVC/NBR blends is matrix shear yielding, irrespective of rubber particle spatial distribution. However, the particle spatial distribution has been experimentally observed to considerably affect the toughness and fracture behaviour of the blends. The blends with the morphology of well-dispersed particles upon impact deform uniformly, while the blends with the pseudonetwork morphology yield preferentially in the pseudonetwork band phase. The pseudonetwork cores deform much less easily than the pseudonetwork bands. The experimental results also confirm that the NBR rubber particles act as stress concentrators to promote shear yielding of PVC respectively in the pseudonetwork bands and in the blends with the morphology of well-dispersed particles. The fractographic analysis on the blends with the above two types of morphologies provides experimental evidence for the suitability of our models for these morphologies that emphasize the roles of rubber particle spatial distribution and matrix ligament thickness.

(Keywords: rubber-toughened poly(vinyl chloride); rubber particle spatial distribution; fracture behaviour)

INTRODUCTION

Brittle ductile transition has been observed in many rubber-toughened plastics[1–26], in $CaCO_3$-toughened polyethylene (PE)[27–29] and kaolin-toughened polypropylene (PP)[30]. The extensive shear yielding and multiple crazing that are able to absorb considerable energy are two important toughening mechanisms[31–33]. The highly localized shear yielding and crazing are, however, considered to lead to brittle fracture[32]. The rubber particles and rigid inorganic fillers dispersed in the plastic matrices act as the stress concentrators to initiate a transition of deformation behaviour of the matrices from highly localized shear yielding or crazing to extensive shear yielding or to multiple crazing. The differences in the fracture behaviour can be examined under the electron microscopy.

It has long been known that the matrix chain structure markedly affects the toughening mechanism[4,31–33]. Polymers that have a high chain entanglement density tend to deform by shear yielding, e.g. polycarbonate, polyamide, polyester, PE and PP. On the other hand, polymers that have a low chain entanglement density tend to deform by crazing, e.g. polystyrene (PS), poly(methyl methacrylate) (PMMA) and poly(styrene-*co*-acrylonitrile) (SAN). Poly(vinyl chloride) (PVC) has an intermediate chain entanglement density. Shear yielding is the main toughening mechanism for PVC toughened by rubber[5].

The brittle ductile transition in polymer blends and composites is governed by the morphological parameters. For a given particle size, it has been observed to occur at a critical particle content[11,27–30]. For a constant particle content, it is also seen at a critical particle size[3,4]. Recently the particle size distribution was demonstrated to be a crucial parameter in determining the critical behaviour[26,29]. It is emphasized that the critical values of particle size and content are functions of the particle size distribution. A wide particle size distribution is unfavourable for the toughening of polymers. However, none of the above parameters are more basic than the matrix ligament thickness (or surface-to-surface interparticle distance). The reason is that a brittle ductile transition master curve can be attained only by plotting impact strength against the matrix ligament

* To whom correspondence should be addressed
† Present address: PO Box 13, Taiyuan 030051, Shanxi, People's Republic of China

thickness[2–5,10,11,26–29] and it is possible to separate the effects of the morphological parameters on toughness from those of other factors by the master curve. An example is the separation of the influence of interfacial adhesion from the effects of the morphological parameters in PVC/nitrile rubber (NBR) blends[34,35].

The particle spatial distribution (spatial packing or dispersion state) is one of the morphological parameters. It has been shown that this factor also considerably influences impact strength[5,12,14–19,36–40]. It is well known that agglomerated rubber particles cannot toughen plastics. Hence, the morphology of well-dispersed particles is usually expected. It should be pointed out that there is another spatial distribution that has a much higher toughening efficiency than the morphology of well-dispersed particles[14–19,36–40], which has been called the pseudonetwork morphology[29,39–43]. This would mean that the particle spatial distribution plays an important role in the rubber toughening of polymers.

In several independent papers[40–43], we have established the models for the pseudonetwork morphology and the morphology of well-dispersed particles. These models are based on the role of stress concentration of dispersed particles that promote the plastic deformation of surrounding polymer matrix. The viability of these models must be verified.

In this work, we investigate the effects of morphological parameters on the fracture behaviour of PVC/NBR blends. To clarify the difference between the pseudonetwork morphology and the morphology of well-dispersed particles and provide our models with experimental evidence, we focus attention on the two types of morphologies. The relation of fracture behaviour to the particle spatial distribution and matrix ligament thickness is presented.

RESULTS AND DISCUSSION

The morphology

The pseudonetwork morphology and the morphology of well-dispersed particles are schematically illustrated in *Figures 1a* and *b*, where the dark dots represent the rubber particles. *Figure 1a* shows the pseudonetwork morphology. The rubber particles are dispersed in a plastic matrix between the pseudonetwork cores (dashed circles). It should be pointed out that there is no limit to the shape of pseudonetwork cores. We give an example of the spherical pseudonetwork cores in *Figure 1a*. *Figure 1b* displays the morphology of well-dispersed particles. The rubber particles are randomly dispersed in a plastic matrix.

It is well known that PVC obtained by suspension polymerization can exhibit three types of particulate structure. The largest structure is the powder grain with a diameter of about 100 μm. The powder grains start to break down into primary particles of about 1 μm in diameter at the lower processing temperatures. The primary particles are fused into the domains ranging from 10 to 100 nm in size at the higher processing temperatures. The particulate nature in the final product relies on the processing aids, processing conditions and PVC molecular weight. The NBR particle spatial distributions in the PVC matrix were controlled at the different stages of PVC powder breakage. The PVC particulate structures are different in the two types of morphologies in this work. For the pseudonetwork morphology, the PVC primary particles between which the NBR particles are distributed are not destroyed. For the morphology of well-dispersed NBR particles, the breakdown of PVC primary particles causes the NBR particles to be scattered randomly in the PVC matrix. The PVC molecular weight, plasticizer, processing temperature and blending time play key roles in the control of rubber particle spatial distributions in this work. The optimum PVC molecular weight and composition for the control of the two types of morphologies have been studied[17]. On the one hand, the primary particles of low-molecular-weight PVC, e.g. lower than about 43 750, were very easily broken down into smaller particulate structure without the addition of plasticizer. In other words, the pseudonetwork morphology was not attained with the low-molecular-weight PVC. On the other hand, the primary particles of high-molecular-weight PVC, e.g. higher than about 81 250, were not completely destroyed even with the addition of some level of plasticizer, for example 5 parts per hundred of resin. This means that the morphology of well-dispersed rubber particles was not achieved with the high-molecular-weight PVC. Thus, the medium-molecular-weight PVC is suitable for the purpose of this study. In this work, the PVC with molecular weight 62 500 is used for all blends (the molecular weight of the above PVC is the number-averaged molecular weight reported by the manufacturer). The PVC/NBR blends with the pseudonetwork morphology (*Figure 2a*) were obtained by blending at lower temperature, shorter blending time and in the absence of plasticizer. The addition of plasticizer, higher processing temperature and longer blending time favour the formation of the morphology of well-dispersed NBR particles (*Figure 2b*).

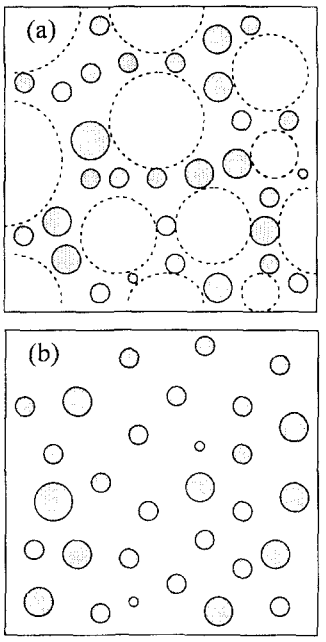

Figure 1 Schematics of particle spatial distribution: (a) pseudonetwork; (b) well-dispersed. The filled symbols and the dashed circles represent the rubber particles and the pseudonetwork cores, respectively. After Ref. 40

Theoretical calculations and experimental measurements[39,41–43] have shown that the toughness of the blends with the pseudonetwork morphology are insensitive to the NBR types, for instance, NBRs a–c (NBRa, a commercial product, was milled for 15 or 30 min at room temperature to obtain NBRb and NBRc). Hence, only the NBRa was used to prepare the PVC/NBR blends with the pseudonetwork morphology. The NBR particle sizes for the blends with the morphology of well-dispersed NBR particles were controlled by NBR molecular weight that results in different viscosity ratio of PVC matrix to rubber. Both the NBR and

Figure 2 Scanning electron micrographs for PVC/NBR blends with (a) the pseudonetwork morphology and (b) the morphology of well-dispersed particles. After Ref. 43

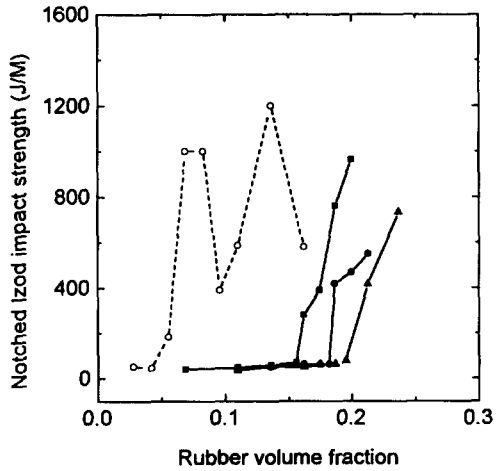

Figure 3 Notched Izod impact strength *versus* rubber volume fraction for PVC/NBR blends with well-dispersed rubber particles (solid symbols) and the pseudonetwork structure (open circles). After Ref. 43

PVC primary particles have been shown to fit log–normal distribution[39–41,43]. The rubber particle size distribution parameter for blends with the two types of morphologies and the PVC primary particle size distribution parameter are in the range from 1.35 to 1.7.

The brittle ductile transition

Figure 3 shows the relation of impact strength to rubber volume fraction for PVC/NBR blends with the two types of morphologies. For the PVC/NBR blends with the morphology of well-dispersed rubber particles (solid lines), a brittle ductile transition is seen to occur at a critical rubber volume fraction. The critical rubber volume fraction increases in the order of NBRs a–c. It has been demonstrated that the critical rubber volume fraction is a function not only of the width of the rubber particle size but also of the rubber particle size distribution. It increases with the rubber particle size and the width of the rubber particle size distribution[26,29,38]. For the PVC/NBR blends with the pseudonetwork morphology (dashed line), the impact strength varies dramatically with the rubber volume fraction. This has been attributed mainly to the change in the morphological parameters of pseudonetwork cores[39–43].

The brittle ductile transition master curves by plotting impact strength *versus* matrix ligament thickness have been obtained in many polymer blends with the morphology of well-dispersed particles, i.e. rubber-toughened nylon[2–5], PP[10,11] and PVC[26,39], and $CaCO_3$-toughened high-density PE[27–29]. These results suggest that the matrix ligament thickness is more important than the rubber particle size, size distribution and volume fraction.

Recently we derived a new equation for the evaluation of matrix ligament thickness (T_r) by[40]

$$T_r = d_r\left[\left(\frac{\pi}{6\phi_r}\right)^{\frac{1}{3}}\exp(1.5\ln^2\sigma_r) - \exp(0.5\ln^2\sigma_r)\right] \quad (1)$$

where d_r, σ_r and ϕ_r are the average rubber particle size, size distribution parameter and volume fraction, respectively. The d_r and ϕ_r are defined by log–normal distribution and are given by[44]

$$\ln d_r = \frac{\sum_{i=1}^{N} n_i \ln d_{r,i}}{\sum_{i=1}^{N} n_i} \quad (2)$$

$$\ln \sigma_r = \left(\frac{\sum_{i=1}^{N} n_i(\ln d_{r,i} - \ln d_r)^2}{\sum_{i=1}^{N} n_i}\right)^{1/2} \quad (3)$$

equation (1) can be used to estimate T_r for the polymer blends with particle size of dispersed phase conforming to log–normal distribution and with the morphology of well-dispersed rubber particles.

For the PVC/NBR blends with the pseudonetwork morphology, equation (1) is, however, invalid. The corresponding T_r can be estimated by[39,41,43]

$$T_r = d_r\left[\xi_r\left(\frac{\pi}{6\phi_r}\right)^{\frac{1}{3}}\exp(1.5\ln^2\sigma_r) - \exp(0.5\ln^2\sigma_r)\right] \quad (4)$$

where ξ_r is given by

$$\xi_r = (1-\phi_P)^{1/3} \quad (5)$$

where ϕ_P is the volume fraction of material that rejects the dispersed particles. Therefore, it is the excluded volume. In this work, it represents the pseudonetwork cores (the PVC primary particles). The NBR particles cannot enter into the PVC primary particle phase. Therefore, the rubber particles are distributed in the fused PVC more closely. The d_r and σ_r in equation (4) are also defined by log–normal distribution.

The ξ_r for the PVC/NBR blends is estimated by[39,41,43]

$$\xi_r = \left\{\frac{\left[\frac{d_r}{d_P} + \exp(0.5\ln^2\sigma_P)\right]^3 - \frac{\pi}{6}\left[\exp(1.5\ln^2\sigma_P)\right]^3}{\left[\frac{d_r}{d_P} + \exp(0.5\ln^2\sigma_P)\right]^3}\right\}^{1/3} \quad (6)$$

where d_P is the PVC primary particle size and σ_P the size distribution parameter. They can be attained from the log–normal distribution plot.

Using equations (1) and (4) we are able to convert *Figure 3* into *Figure 4*, which shows the plot of impact strength *versus* matrix ligament thickness. Clearly, one brittle ductile transition master curve cannot be attained owing to the effect of rubber particle spatial distribution on impact strength[39,41,43]. The ξ_r values for the PVC/NBR blends with the pseudonetwork morphology are smaller than one and are not a constant. They range from 0.69 to 0.85 in this work, indicating that their differences are not great. Thus we are able to approximately obtain a master curve. The critical value (T_{rc1}) of T_r for the PVC/NBR blends with the pseudonetwork morphology is 0.11 μm. A blend is tough if $T_r < T_{rc}$. A blend is brittle if $T_r > T_{rc}$. For the PVC/NBR blends with the morphology of well-dispersed particles, a master curve (solid line) is seen. The brittle ductile transition takes place at the critical value (T_{rc2} = 0.059 μm) of T_r. In the T_r range from 0.059 to 0.11 μm, the impact strength for the PVC/NBR blends with the pseudonetwork morphology is greater than that for the PVC/NBR blends with the morphology of well-dispersed particles. The dependence of impact strength on the rubber particle spatial distribution seems to disappear when T_r is very small, for instance, smaller than 0.053 μm.

Thus, both the particle spatial distribution and the matrix ligament thickness are interdependent factors for the brittle ductile transition of polymer blends. In other words, the brittle ductile transition master curve is a function of particle spatial distribution.

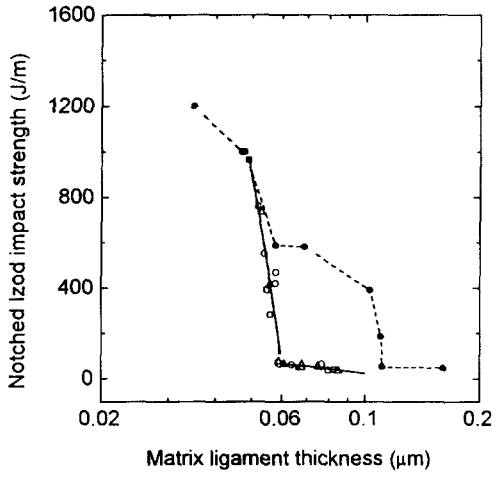

Figure 4 Notched Izod impact strength *versus* matrix ligament thickness for PVC/NBR blends with well-dispersed rubber particles (open symbols) and the pseudonetwork structure (solid circles). After Ref. 43

Fractographic analysis

Izod impact tests were carried out according to ASTM-D256 but at 16°C. The fracture surfaces were then coated with Au. The fractographs were observed on a Hitachi S-530 scanning electron microscope. The fracture surfaces typically for clarifying the influences of T_r and ξ_r on fracture behaviour were examined by scanning electron microscopy (SEM). It is known that the fractographs could be different for different fracture processes, which are the crack initiation and propagation[32,45] and termination of a crack because of very high impact resistance. Therefore, the fracture surfaces are roughly divided into three regions illustrated in *Figure 5*. The region A is near the notch, where the crack is initiated. The region B is in the centre of the fracture surface, where the crack propagates. The region C near the region B is far away from the region A, where the crack propagates or might be terminated depending on the toughening effect. The corresponding SEM pictures are taken in these regions.

We first analyse the fractographs of brittle blends. The samples with different values of T_r and ξ_r were examined. The samples whose values of T_r are slightly smaller than $T_{r,c1}$ and $T_{r,c2}$ are interesting since stress whitening begins to occur in the region A. The fracture patterns in regions B and C for these brittle PVC/NBR blends are similar because the crack propagates in both regions. Consequently, the results in region B are given here. The impact strength, T_r and ξ_r for the blend with the pseudonetwork morphology are 53 J m^{-1}, 0.11 μm (= $T_{r,c1}$) and 0.839, respectively. The corresponding values for the blend with the morphology of well-dispersed rubber particles are 68 J m^{-1}, 0.059 μm (= $T_{r,c2}$) and 1. Compared to the pure PVC, the increase of impact strength (see *Table 1*) for the two blends is attributable mainly to the energy absorbed in the crack initiation process, which exhibits localized plastic deformation. The fracture process is then followed by the crack propagation without termination in the two blends. In general, there is no significant difference in the impact strength arising from the change in T_r and ξ_r since the two blends are brittle. *Figures 6* and *7* are the SEM pictures taken in the regions A and B. *Figures 6a* and *b* show the results for the blend with the

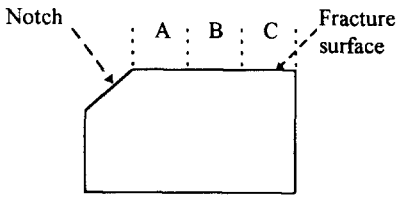

Figure 5 Schematic illustration of SEM fractographs taken in regions (A) near the notch, (B) in the centre of fracture surface and (C) near the region B but away from the region A

Table 1 Impact strength and morphological parameters for PVC/NBR blends with the pseudonetwork morphology and with the morphology of well-dispersed rubber particles (data taken from Ref. 43)

Blend	Impact strength (J m^{-1})	Morphological parameters						
		ϕ_r	d_r (μm)	σ_r	d_P (μm)	σ_P	ξ_r	T_r (μm)
A	53	0.028	0.076	1.32	0.45	1.36	0.839	0.11
B	68	0.116	0.073	1.48			1	0.059
C	1000	0.059	0.059	1.4	0.38	1.61	0.74	0.048
D	413	0.213	0.109	1.37			1	0.056
Pure PVC	30							

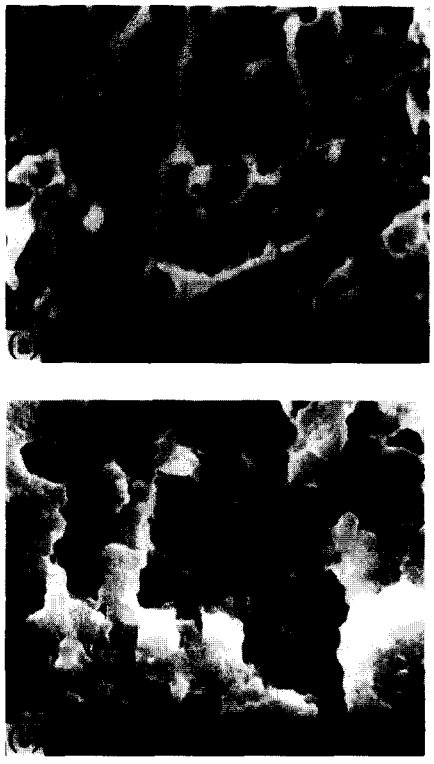

Figure 6 Fractographs for a brittle PVC/NBR blend with the pseudonetwork morphology taken in (a) the region A and (b) the region B

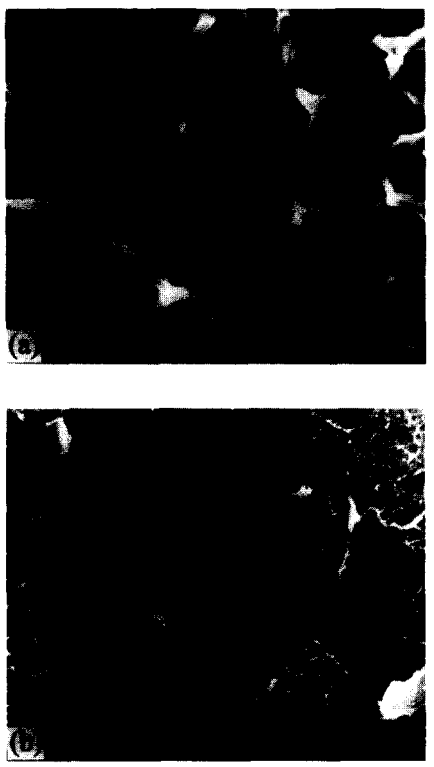

Figure 7 Fractographs for a brittle PVC/NBR blend with the morphology of well-dispersed particles taken in (a) the region A and (b) the region B

pseudonetwork morphology. Fibrils and voids leading to stress whitening are seen in *Figure 6a* taken in the region A, indicating localized plastic deformation. However, there is no observed fibril and void in the regions B and C. *Figures 7a* and *b* show the results for the blend with the morphology

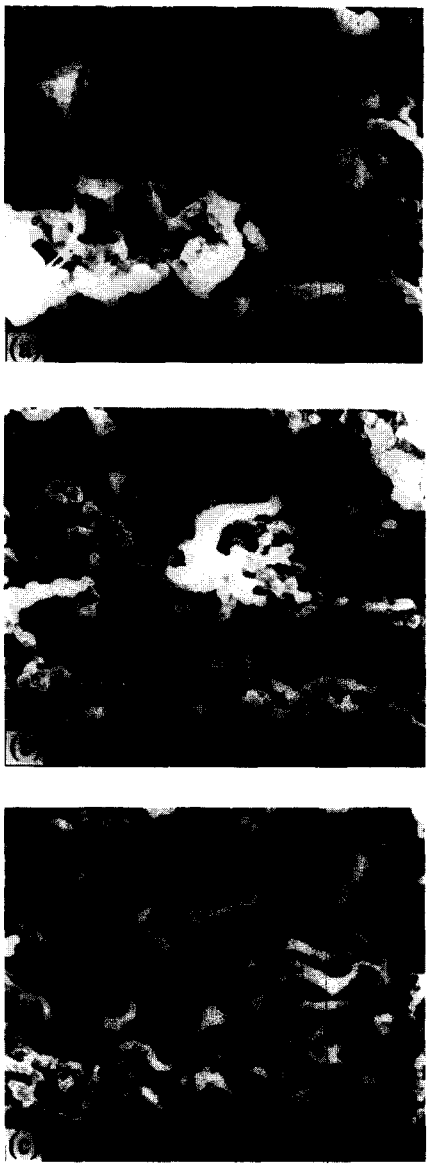

Figure 8 Fractographs for a tough PVC/NBR blend with the pseudonetwork morphology taken in (a) the region A, (b) the region B and (c) the region C

of well-dispersed NBR particles. Stress whitening is obvious in the region A owing to the formation of large numbers of voids. Fibrils are also evident in this region. The localized fibrils are seen in the region B shown in *Figure 7b*. Comparing *Figure 6* with *Figure 7*, one may find a marked difference in the deformation behaviour. The PVC matrix yields uniformly in *Figure 7a*, but a lot of PVC primary particles have not yet deformed in *Figure 6a*.

We then analyse the fractographs of tough blends. The SEM pictures in regions A, B and C are presented. *Figure 8* shows the fracture surfaces of the PVC/NBR blend with the pseudonetwork morphology. The sample is extremely tough and was not broken completely. The impact strength, T_r and ξ_r for the blend given in *Table 1* are 1000 J m^{-1}, 0.048 μm ($< T_{r,cl}$) and 0.74, respectively. Fibrils, voids and undeformed PVC primary particles are seen in the region A shown in *Figure 8a*, which is similar to *Figure 6a*. The fracture surface in region B shown in *Figure 8b* resembles that in region A, but is different from that shown in *Figure 6b*. In region B the crack propagation is hindered but not terminated. The plastic deformation in region C

Figure 9 Fractographs for a tough PVC/NBR blend with the morphology of well-dispersed particles taken in (a) the region A, (b) the region B and (c) the region C

becomes much more intense as shown in *Figure 8c*. In this region the crack is stopped. From the initiation to termination of the crack, considerable energy is absorbed resulting in very high toughening efficiency due to the reduction of T_r and ξ_r (see also *Table 1*). *Figure 9* shows the fracture surfaces of the PVC/NBR blend with the morphology of well-dispersed rubber particles. The blend is also very tough and was not broken completely. The impact strength, T_r and ξ_r for the blend given in *Table 1* are 413 J m^{-1}, 0.056 μm ($< T_{r,c2}$) and 1, respectively. The three fracture processes similar to those of the tough blend with the pseudonetwork morphology take place in the tough blend with the morphology of well-dispersed rubber particles. The corresponding fractographs are shown in *Figures 9a–c*. Fibrils and voids are seen in regions A–C but without undeformed PVC primary particles. The fractographs in the regions B and C differ from those observed in *Figure 7b*.

Breuer and co-workers[36,37] also examined the damage region under the fracture surface of rubber toughened PVC. Siegmann and Hiltner[45] studied the toughening mechanisms of rubber toughened PVC by observing the fracture surfaces. They concluded that matrix shear yielding is the main energy absorption mechanism. The SEM observations on the fracture surfaces PVC/NBR blends presented here confirm their conclusion. The above experimental results also show that the particle spatial distribution does not affect the toughening mechanism of the blends. For blends with the above two types of morphologies, the toughening mechanism is matrix shear yielding.

The analysis of the fractographs and corresponding fracture processes suggests that the pseudonetwork morphology is different from that of well-dispersed rubber particles. The pseudonetwork cores (the PVC primary particles) play a crucial role in the toughening of PVC. They deform less easily than the pseudonetwork bands consisting of NBR particles and fused PVC. The rubber particles are packed more closely in the blend with the pseudonetwork morphology when the particle size, size distribution and volume fraction are identical, as predicted by equation (4). In the T_r range from $T_{r,c2}$ to $T_{r,c1}$, the impact strength for the blends with the pseudonetwork morphology is much higher than that for the blends with the morphology of well-dispersed particles, indicating that the impact strength is also a function of ξ_r. As a result, the toughening effect of the pseudonetwork morphology is considerably stronger than that of the morphology of well-dispersed particles.

CONCLUSIONS

The particle spatial distribution has been experimentally observed to considerably affect the toughness of polymer blends. This has been simulated by our models for the morphology of well-dispersed particles and the pseudonetwork morphology. The difference in these models for the two types of morphologies is that the equation for calculating the matrix ligament thickness of blends with the pseudonetwork morphology contains the spatial distribution factor ξ_r to which the pseudonetwork cores contribute. The particles in blends with this morphology are distributed more closely due to the excluded volume of pseudonetwork cores. The smaller the ξ_r, the smaller the matrix ligament thickness. Moreover, the toughness is not only a function of matrix ligament thickness but also a function of ξ_r. The smaller the ξ_r, the tougher the blend.

The fractographic analysis of PVC/NBR blends with the above two types of morphologies provides experimental evidence for the suitability of our models for these morphologies. The blends with the morphology of well-dispersed particles upon impact deform uniformly. Conversely, the blends with the pseudonetwork morphology yield preferentially in the pseudonetwork band phase. The pseudonetwork cores deform with much more difficulty compared to the pseudonetwork bands.

The above experimental results also confirm that the NBR rubber particles act as stress concentrators to promote shear yielding of PVC respectively in the pseudonetwork bands and in the blends with the morphology of well-dispersed particles. Therefore, the particle spatial distribution does not affect the toughening mechanism of the blends.

ACKNOWLEDGEMENTS

This work was supported by the NSFC (China) through Grant 59233060 and the Hong Kong Research Grant Council.

REFERENCES

1. Hobbs, S. Y., Bopp, R. C. and Watkins, V. H., *Polym. Eng. Sci.*, 1983, **23**, 380.
2. Flexman, E. A., *Mod. Plast.*, 1985, **62**, 72.
3. Wu, S., *Polymer*, 1985, **26**, 1855.
4. Wu, S., *Polym. Eng. Sci.*, 1990, **30**, 753.
5. Wu, S., *J. Appl. Polym. Sci.*, 1988, **35**, 549.
6. Borggreve, R. J. M., Gaymans, R. J., Schuijer, J. and Ingen Housz, J. F., *Polymer*, 1987, **28**, 1489.
7. Borggreve, R. J. M., Gaymans, R. J. and Schuijer, J., *Polymer*, 1989, **30**, 71.
8. Borggreve, R. J. M., Gaymans, R. J. and Eichenwald, H. M., *Polymer*, 1989, **30**, 78.
9. Borggreve, R. J. M. and Gaymans, R. J., *Polymer*, 1989, **30**, 63.
10. Jancar, J., DiAnselmo, A. and DiBenedetto, A. T., *Polym. Commun.*, 1991, **32**, 367.
11. Wu, X., Zhu, X. and Qi, Z., Proceedings of the 8th International Conference on Deformation, Yield and Fracture of Polymers, London, 1991, p. 78/1.
12. Aoki, Y. and Watanabe, M., *Polym. Eng. Sci.*, 1992, **33**, 748.
13. Gloaguen, J. M., Steer, P., Gailland, P., Wrotecki, C. and Lefebver, J. M., *Polym. Eng. Sci.*, 1993, **33**, 748.
14. Keskkula, H., Kim, H. and Paul, D. R., *Polym. Eng. Sci.*, 1990, **30**, 1373.
15. Kim, H., Keskkula, H. and Paul, D. R., *Polymer*, 1990, **31**, 869.
16. Majumdar, B., Keskkula, H. and Paul, D. R., *Polymer*, 1994, **35**, 3164.
17. Majumdar, B., Keskkula, H. and Paul, D. R., *Polymer*, 1994, **35**, 5453.
18. Majumdar, B., Keskkula, H. and Paul, D. R., *Polymer*, 1994, **35**, 5468.
19. Brady, A. J., Keskkula, H. and Paul, D. R., *Polymer*, 1994, **35**, 3665.
20. Dompas, D. and Groeninckx, G., *Polymer*, 1994, **35**, 4743.
21. Dompas, D., Groeninckx, G., Isogawa, M., Hasegawa, T. and Kadokura, M., *Polymer*, 1994, **35**, 4750.
22. Dompas, D., Groeninckx, G., Isogawa, M., Hasegawa, T. and Kadokura, M., *Polymer*, 1994, **35**, 4760.
23. Liu, N. C. and Baker, W. E., *Polym. Eng. Sci.*, 1992, **32**, 1695.
24. Angola, J. C., Fujita, Y., Sakai, T. and Inoue, T., *J. Polym. Sci. Polym. Phys. Ed.*, 1988, **26**, 807.
25. Liu, N. C. and Baker, W. E., *Polymer*, 1994, **35**, 988.
26. Liu, Z. H., Zhu, X. G, Zhang, X. D., Qi, Z. N. and Wang, F. S., *Acta Polymerica Sinica*, 1996, (4), 468.
27. Fu, Q., Wang, G. and Shen, J., *J. Appl. Polym. Sci.*, 1993, **49**, 1985.
28. Liu, C. X., M.S. thesis, Chengdu University of Science and Technology, Chengdu, 1992.
29. Liu, Z. H., Zhu, X. G., Li, Q., Qi, Z. N. and Wang, F. S., *Polymer*, 1998, **39**, 1863.
30. Ou, Y. C., Fang, X. P., Shi, H. Q. and Feng, Y. P., *Acta Polymerica Sinica*, 1996, (1), 59.
31. Bucknall, C. B., *Toughened Plastics*. Applied Science, London, 1977.
32. Kinloch, A. J. and Young, J., *Fracture Behaviour of Polymers*. Applied Science, London, 1983.
33. Kausch, H. H., *Crazing in Polymers*. Springer, Berlin, 1983.
34. Liu, Z. H., Zhu, X. G., Zhang, X. D., Qi, Z. N., Wang, F. S. and Choy, C. L., Effect of interfacial adhesion on the toughness and toughening mechanisms of PVC/NBR blends, in *Proceedings of 1st East Asian Polymer Conference*, 11–15 October 1995, Shanghai, P.R. China, p. 80.
35. Liu, Z. H., Zhu, X. G., Zhang, X. D., Qi, Z. N., Wang, F. S. and Choy, C. L., *Acta Polymerica Sinica*, 1997, (3), 283.
36. Breuer, H., Haaf, F. and Stabenow, J., *J. Macromol. Sci. Phys.*, 1977, **B14**, 387.
37. Haaf, F., Breuer, H. and Stabenow, J., *Angew. Makromol. Chem.*, 1977, **58/59**, 95.
38. Ryan, C. F. and Jalbert, R. L., in *Encyclopedia of PVC*, Vol. 2, ed. L. I. Nass. Dekker, New York, 1976.
39. Liu, Z. H., Ph.D. thesis, Institute of Chemistry, Chinese Academy of Sciences, Beijing, 1994.
40. Liu, Z. H., Zhang, X. D., Zhu, X. G., Qi, Z. N. and Wang, F. S., *Polymer*, 1997, **38**, 5267.
41. Liu, Z. H., Zhu, X. G., Zhang, X. D., Qi, Z. N., Choy, C. L. and Wang F. S., *Acta Polymerica Sinica*, 1998, (**1**), 8.
42. Liu, Z. H., Zhu, X. G., Zhang, X. D., Qi, Z. N., Choy, C. L. and Wang F. S., *Acta Polymerica Sinica*, 1997, (**5**), 565.
43. Liu, Z. H., Zhang, X. D., Zhu, X. G., R. K. Y. Li, Qi, Z. N., Wang, F. S. and Choy, C. L., *Polymer*, accepted.
44. Irani, R. R. and Callis, C. F., *Particle Size: Measurement, Interpretation and Application*. Wiley, New York, 1963.
45. Siegmann, A. and Hiltner, A., *Polym. Eng. Sci.*, 1984, **24**, 869.